SUBGRID-SCALE MODELING OF TURBULENT HEAT TRANSPORT IN FORCED CONVECTION AT HIGH MOLECULAR PRANDTL NUMBERS

Irrenfried C. and Steiner H.*
*Author for correspondence
Institute of Fluid Mechanics and Heat Transfer,
Graz University of Technology,
Austria,
E-mail: helfried.steiner@tugraz.at

ABSTRACT

Assuming strong similarity between the transport of momentum and heat is a common feature of most standard subgrid-scale models used in Large-Eddy Simulations (LES) of turbulent flow with heat transfer. In view of the limitation of this analogy to molecular Prandtl numbers near unity the present study investigates the capability of different established model concepts in predicting the subgrid-scale heat flux, when applied in *a priori* LES of turbulent heated flow going well beyond this parameter range, considering Prandtl numbers $Pr = 1/10/20$ at Reynolds number $Re_\tau = 360$. The test unveils the major deficits of the constant-coefficent Smagorinsky approach due to the non-universiality of the used model coefficients like the turbulent subgrid-scale Prandtl number. Apart from the removal of this basic shortcoming the dynamic Smagorinsky model is shown to yield no substantially better predictions. The same holds true for the computationally more elaborate non-linear extensions introducing a tensorial diffusivity. The scale-similarity based mixed dynamic model proposed by [1] was proven to give in general the most accurate description. Some discrepancy appeared in regions with considerable net transfer of heat from the unresolved into the smallest resolved scales observed for higher Prandtl number. This suggests to include a sub-model for the presently neglected cross-scale interaction into the formulation as path for further improvement of this best evaluated approach.

INTRODUCTION

The increasingly strong discrepancy between the small scale convective fluxes of momentum and heat associated with the break-down of the Reynolds analogy at increasingly high molecular Prandtl numbers still poses a great challenge to the modelling of the unresolved subgrid-scale heat flux in Large-Eddy simulation. Most modelling approaches, such as the widely used Smagorinsky-type linear eddy-diffusivity models, their more advanced non-linear extensions, or scale-similarity based alternative models, have been thus far mainly evaluated for molecular Prandtl numbers fairly close to unity. The present work puts the focus on this issue. In the first step, several Direct Numerical Simulations (DNS) of heated turbulent pipe flow are carried out at wall friction Reynolds number $Re_\tau = 360$ varying the Prandtl number up to $Pr = 20$. The obtained instantaneous solutions are further used in *a priori* tests of various simple as well as more advanced subgrid-scale models proposed in literature to investigate their scope and limits und in the considered parameter range.

NOMENCLATURE

A^+	[-]	Van Driest constant
a	$[m^2/s]$	thermal diffusivity
a_T	$[m^2/s]$	eddy diffusivity
C_S	[-]	Smagorinsky constant
$C_W, C_N, C_{\Theta,j}$	[-]	*NLM* model parameter
K, h	[-]	*DTM* model parameter
p	$[Pa]$	pressure
Pr	[-]	molecular Prandtl number
Pr_T	[-]	turbulent subgrid-scale Prandtl number
q_j	$[mK/s]$	subgrid-scale heat flux
Q_j	$[mK/s]$	subgrid-scale heat flux on test-filter level
Re_τ	[-]	friction Reynolds number
S_{ij}	$[s^{-1}]$	strain-rate tensor
t	$[s]$	time
T	$[K]$	temperature
T_{ij}	$[s^{-1}]$	subgrid-scale stress on test-filter level
u_j	$[m/s]$	velocity component
w_τ	$[m/s]$	wall friction velocity
x_i	$[m]$	coordinate in diretion i

Abbreviations

CSM	Constant coefficient Smagorinsky model
DNS	Direct numerical simulation
DSM	Dynamic Smagorinsky model
DTM	Dynamic two-parameter model
LES	Large eddy simulation
NLM	Non-linear tensorial viscosity/diffusivity model
SGS	Sub-grid scale

Special characters

δ_{ij}	[-]	Kronecker Delta
$\overline{\Delta}, \widehat{\Delta}$	$[m]$	grid/test-filter width
ν	$[m^2/s]$	kinematic viscosity
ν_T	$[m^2/s]$	eddy viscosity
Ω_{ij}	$[s^{-1}]$	rotation rate tensor
ρ	$[kg/m^3]$	density
τ_{ij}	$[m^2/s^2]$	subgrid-scale stress

Subscripts and Superscripts

$()^+$	scaled in wall coordiantes
$\underline{()}^d$	deviatoric part of tensor
$\overline{()}$	filtered representation
$()'$	unresolved contribution
$<>$	statistically averaged

FILTERED GOVERNING EQUATIONS

Assuming incompressible flow the spatially filtered conservation equations of mass, momentum and energy, which are solved by Large-Eddy Simulation (LES), read

$$\frac{\partial \overline{u}_j}{\partial x_j} = 0 \tag{1}$$

$$\frac{\partial \overline{u}_i}{\partial t} + \frac{\partial \overline{u}_i \overline{u}_j}{\partial x_j} = -\frac{1}{\rho}\frac{\partial \overline{p}}{\partial x_i} + \nu \frac{\partial^2 \overline{u}_i}{\partial x_j \partial x_j} - \frac{\partial \tau_{ij}}{\partial x_j} \tag{2}$$

$$\frac{\partial \overline{T}}{\partial t} + \frac{\partial \overline{T}\,\overline{u}_j}{\partial x_j} = a \frac{\partial^2 \overline{T}}{\partial x_j \partial x_j} - \frac{\partial q_j}{\partial x_j}, \tag{3}$$

where appropriate subgrid-scale models are needed to close the unresolved stresses and heat fluxes,

$$\tau_{ij} = \overline{u_i\, u_j} - \overline{u}_i\, \overline{u}_j \tag{4}$$

$$q_j = \overline{u_j\, T} - \overline{u}_i\, \overline{T}, \tag{5}$$

respectively. The present work particularly focuses the modelling of the latter, which is therefore analyzed here in some more detail. Adopting the classical decomposition introduced by [2] for the subgrid-scale stress tensor, the subgrid-scale heat flux defined in (5) can be decomposed into

$$q_j = q_j^L + q_j^C + q_j^R. \tag{6}$$

These three terms represent the heat flux analogue of the Leonard stress, the cross-stress and the Reynolds stress tensor, respectively, and they read

$$\text{Leonard heat flux: } q_j^L = \overline{\overline{u_j}\,\overline{T}} - \overline{\overline{u_j}}\,\overline{\overline{T}} \tag{7}$$

$$\text{Cross heat flux: } q_j^C = \overline{u_j'\,\overline{T}} + \overline{\overline{u_j}\,T'} - \overline{u_j'}\,\overline{\overline{T}} - \overline{\overline{u_j}}\,\overline{T'} \tag{8}$$

$$\text{Reynolds heat flux: } q_j^R = \overline{u_j'\,T'} - \overline{u_j'}\,\overline{T'} \tag{9}$$

As seen from their definition, the Leonard heat flux represents the interaction between the resolved scale fluxes, the cross heat flux the interaction between the smallest resolved and unresolved scale fluxes, and the Reynolds heat flux denotes the interaction between the unresolved scale fluxes. The majority of the subgrid-scale models do not distinguish between these different types of interaction, and simply model the subgrid-scale flux q_j as total. The following section gives a short overview of the subgrid-scale models to be presently examined in *a priori* tests.

SUBGRID-SCALE MODELS

Boussinesq-type linear eddy/diffusivity concept

This most popular concept models the deviatoric components of the subgrid-scale stresses and the heat fluxes analogously to their diffusive counterparts as

$$\tau_{ij}^d = \tau_{ij} - \frac{\delta_{ij}}{3}\tau_{kk} = -2\nu_T \overline{S}_{ij} \tag{10}$$

$$q_j = -a_T \frac{\partial \overline{T}}{\partial x_j} = -\frac{\nu_T}{Pr_T}\frac{\partial \overline{T}}{\partial x_j}, \tag{11}$$

respectively, introducing the eddy viscosity ν_T and eddy diffusivity a_T as turbulent transport coefficients, which have to be determined. The classical constant-coefficient Smagorinsky model [3] computes the eddy viscosity and eddy diffusivity as

$$\nu_T = (C_S\overline{\Delta})^2 |\overline{S}|, \quad a_T = \frac{\nu_T}{Pr_T}, \tag{12}$$

respectively, where C_S is the Smagorinsky constant, $\bar{\Delta}$ a filter-width representative for the resolved grid-scale, $|\overline{S}| = (2\overline{S}_{ij}\,\overline{S}_{ij})^{1/2}$ is the norm of the resolved strain-rate tensor, and Pr_T is the subgrid-scale Prandtl number. One major drawback of this approach is due to the fact that the model coefficients are not universal, but vary from case to case. For wall-bounded flows a VanDriest-type wall-damping function [4] is mostly incorporated in (12), such that the eddy viscosity, rewritten as

$$\nu_T = \left(C_S\overline{\Delta}\right)^2 \left[1 - exp\left(-\frac{y^+}{A^+}\right)\right]^2 |\overline{S}|, \tag{13}$$

vanishes near solid walls, as the non-dimensional wall distance y^+ goes to zero. The dynamic Smagorinsky model was proposed by [5] in order to avoid the conceptual shortcomings of the constant-coefficient approach. The dynamic procedure applies the Smagorinsky ansatz (12) to determine the unresolved stresses and heat fluxes on the grid-filter level,τ_{ij} and q_j, and on a coarser "test-filter"-level, T_{ij} and Q_j, associated with a larger filter width $\widehat{\overline{\Delta}} > \overline{\Delta}$. They can be related to each other introducing the so-called Germano identities

$$T_{ij} - \widehat{\tau_{ij}} = \widehat{\overline{u_i}\,\overline{u_j}} - \widehat{\overline{u}_i}\,\widehat{\overline{u}_j}, \tag{14}$$

$$Q_j - \widehat{q_j} = \widehat{\overline{u_j}\,\overline{T}} - \widehat{\overline{u}_j}\,\widehat{\overline{T}}, \tag{15}$$

which depend only on resolved quantities, and are solved for the model coefficients C_S and Pr_T upon substitution of the ansatzes (10) and (11) together with (12).

Non-linear tensorial viscosity/diffusivity models (*NLM*)

As seen from (10) and (11) the linear model concept inherently assumes that the principal axes of the subgrid-scale stress tensor are aligned with the principal axes of the resolved strain-rate tensor, $\tau_{ij} \sim \overline{S}_{ij}$, and that the subgrid-scale heat flux is aligned with the resolved temperature gradient, i.e., $q_j \sim \partial\overline{T}/\partial x_j$, which is both physically not justified. This shortcoming motivated to develop non-linear extensions of the classical Boussinesq-type linear concept in terms of tensor-polynomial models as, e.g., proposed by [6]. They modelled the subgrid-scale stresses and heat fluxes as

$$\begin{aligned}\tau_{ij}^d = &-2(C_S\overline{\Delta})^2|\overline{S}|\overline{S_{ij}} - 4C_W\overline{\Delta}^2\left(\overline{S_{ik}}\,\overline{\Omega_{kj}} + \overline{S_{jk}}\,\overline{\Omega_{ki}}\right)\\ &- 4C_N\overline{\Delta}^2\left(\overline{S_{ik}}\,\overline{S_{kj}} - \overline{S_{mn}}\,\overline{S_{nm}}\frac{\delta_{ij}}{3}\right)\end{aligned} \tag{16}$$

$$q_j = -2C_{\Theta E}\overline{\Delta}^2|\overline{S}|\frac{\partial\overline{T}}{\partial x_j} - C_{\Theta S}\overline{\Delta}^2\overline{S_{jk}}\frac{\partial\overline{T}}{\partial x_k}, \tag{17}$$

where $\overline{\Omega}_{ij} = (\partial\overline{u}_i/\partial x_j - \partial\overline{u}_j/\partial x_i)/2$ represents the resolved rotation rate tensor. The model coefficients C_S, C_W, C_N, as well as $C_{\Theta E}$ and $C_{\Theta E}$ are again determined with a dynamic procedure using the subgrid-scale stresses and fluxes obtained on a coarser test-filter level.

Scale-similarity concept

This concept originally proposed by [7] is based on the assumption, that the dynamics of the smallest resolved eddies is similar to that of the biggest unresolved eddies. It is often used in combination with eddy viscosity/diffusivity models as suggested by [8] to provide sufficiently high dissipation for the unresolved scales. [1] adopted this mixed model approach and proposed the following dynamic two-parameter model (DTM)

$$\tau_{ij}^d = \tau_{ij} - \frac{\delta_{ij}}{3}\tau_{kk} = -2(C_S\overline{\Delta})^2|\overline{S}|\overline{S}_{ij} + K\left(L_{ij}^m - \frac{\delta_{ij}}{3}L_{kk}^m\right) \quad (18)$$

with the Leonard tensor $L_{ij}^m = \overline{\overline{u_i}\,\overline{u_j}} - \overline{\overline{u_i}}\,\overline{\overline{u_j}}$ representing the resolved part of the subgrid-scale stress. The subgrid-scale heat flux vector is modelled as

$$q_j = -\frac{(C_S\overline{\Delta})^2|\overline{S}|}{Pr_T}\frac{\partial\overline{T}}{\partial x_j} + hq_j^L \quad (19)$$

with $q_j^L = \overline{\overline{u_j}\,\overline{T}} - \overline{\overline{u_j}}\,\overline{\overline{T}}$ representing the resolved part of the subgrid-scale heat flux. The model coefficients C_S, K, Pr_T, and h are obtained using a Germano-type dynamic procedure.

DIRECT NUMERICAL SIMULATIONS

Direct Numerical Simulations (DNS) were carried out to generate a fully resolved data base for further use in *a priori* LES. The DNS considered three cases of turbulent pipe flow with constant wall heat flux assuming always $Re_\tau = 360$ and varying $Pr = 1/10/20$. The governing conservation equations, rewritten in cylindrical coordinates, were spatially dicretized with a 4^{th} order accurate Finite-Volume scheme and integrated in time using a 2^{nd} order accurate Adams-Bashforth scheme. The computational mesh contains $256 \times 256 \times 512$ cells into the radial, azimuthal and axial direction, respectively. It is clustered in the radial direction, so that the minimum cell size near the wall is $\Delta y_{min}^+ = 0.256$, $R^+\Delta\phi = 4.418$ and $\Delta z^+ = 3.516$, and the maximum cell in radial direction is $\Delta y_{max}^+ = 2.569$. As such, the applied spatial resolution is comparable to that in recent DNS presented by [9], [10], and [11]. Periodic boundary conditions are used for all dependent variables in the circumferential direction φ. No-slip and no-jump boundary conditions were prescribed for the velocities and temperature at the wall of the pipe at $r/D = 0.5$, respectively. Considering hydro-dynamically and thermally fully developed flow periodic boundary conditions are imposed for the velocities, pressure fluctuations, and the temperature in the axial direction $z^* = z/L$.

A PRIORI TESTS

In the present tests the *a priori* LES data were obtained by filtering the DNS data using a top-hat filter, whose filter width relative to the DNS mesh size was $\overline{\Delta}/\Delta_{DNS} = 4$. The test-filtering, which is applied in the two homogeneous directions (azimuthal- and axial-direction) in the dynamic procedures, uses a top-hat filter with a relative filter-width $\widehat{\overline{\Delta}}/\Delta_{DNS} = 8$, implying a LES-grid-filter to test-filter ratio $\widehat{\overline{\Delta}}/\overline{\Delta} = 2$. Figures (1)-(2) show the mean radial variations of the unresolved subgrid-scale contributions to the total turbulent radial normal and shear stress, and to the total turbulent axial and radial heat flux, respectively, as obtained with the presently applied relative LES-grid-filter setting, always normalized with the corresponding wall fluxes τ_w and q_w, respectively. The unresolved stresses reach evidently at maxiumum about 7% of the total values. The maximum unresolved fraction of the total turbulent heat fluxes increases for increasing Prandtl number, going beyond 20%, as seen by the variation of q_z^+ relative to $q_{z,tot}^+$ for $Pr = 20$ in figure (2).

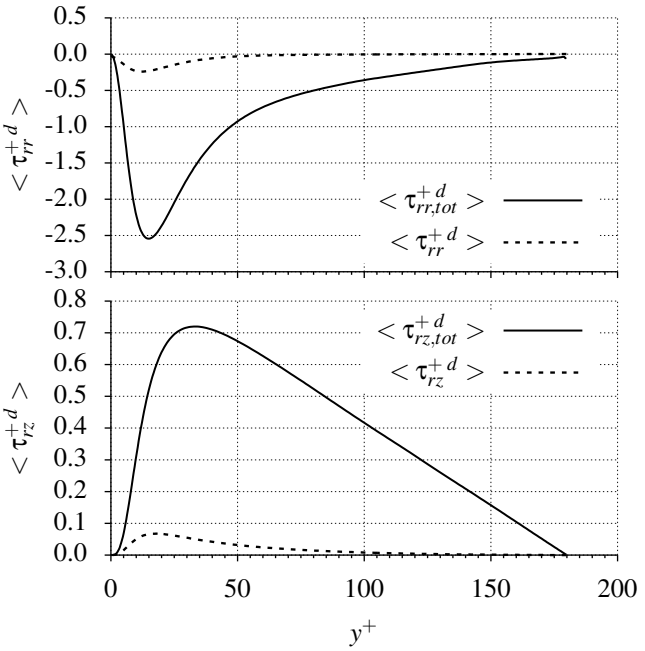

Figure 1. Total and unresolved stresses: deviatoric normal radial stress $\langle\tau_{rr}^{+,d}\rangle$ and shear stress component $\langle\tau_{rz}^{+}\rangle$

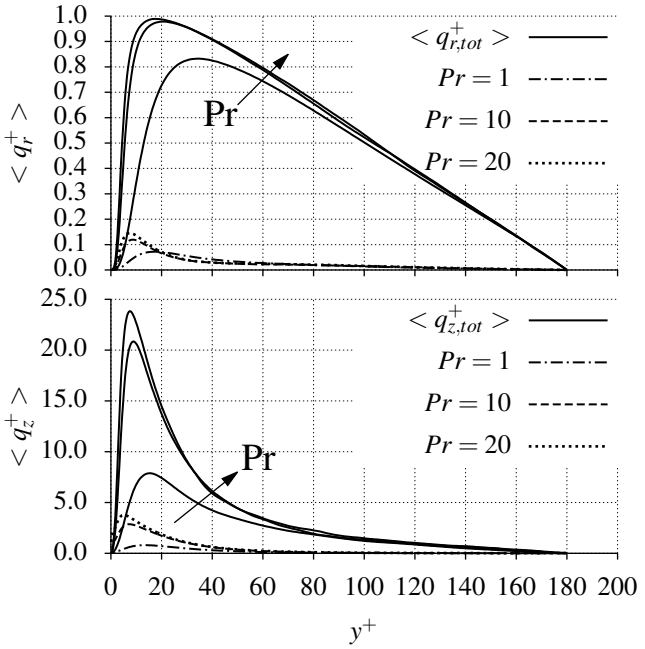

Figure 2. Total and unresolved heat flux: radial $\langle q_r^+\rangle$ and axial $\langle q_z^+\rangle$ component

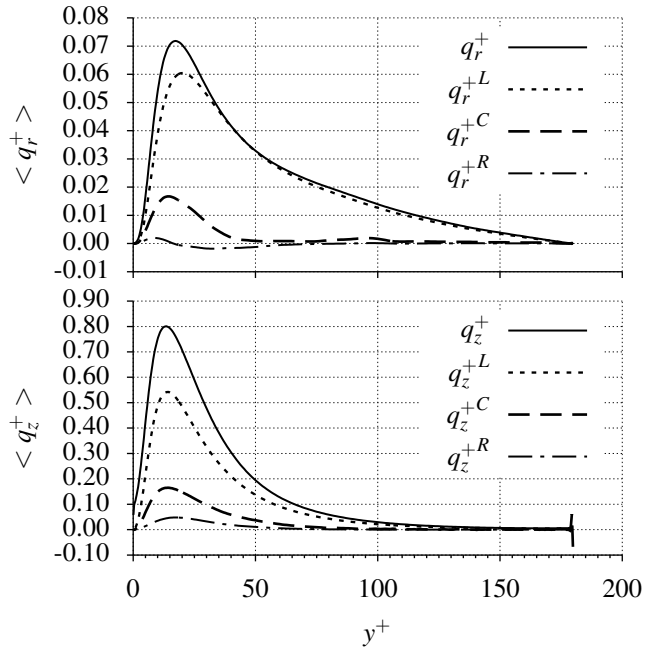

Figure 3. Decomposition of the subgrid-scale fluxes $\langle q_r^+ \rangle$ and $\langle q_z^+ \rangle$ into Leonard, Cross, and Reynolds contributions for $Pr = 1$

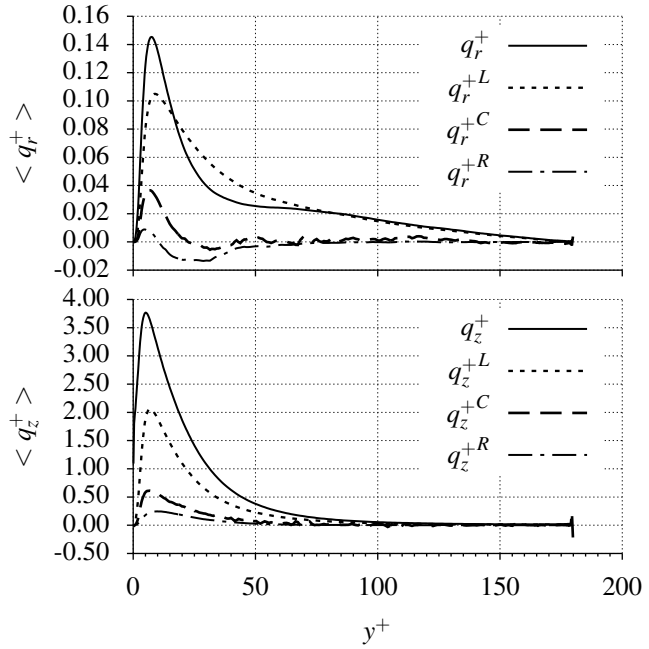

Figure 4. Decomposition of the subgrid-scale fluxes $\langle q_r^+ \rangle$ and $\langle q_z^+ \rangle$ into Leonard, Cross, and Reynolds contributions for $Pr = 20$

Figures (3) and (4) show the radial variations of the mean contribution of the Leonard, Cross, and Reynolds heat fluxes, as defined in equation (6) to the total radial and axial subgrid-scale heat fluxes for $Pr = 1$ and $Pr = 20$. The Leonard term makes evidently up a major part of the total subgrid-scale fluxes, which basically speaks in favor of the subgrid-scale models using such a term in the context of the scale-similarity hypothesis. However, the variations of the radial component of the cross term q_r^{+C} show a significant difference for the two Prandtl numbers. For the high Prandtl number, Pr=20, the cross heat flux becomes negative in the region around $y^+ = 50$. Together with the also negative Reynolds contribution q_r^{+R} this effectively reduces the total subgrid-scale heat flux in this region. This kind of "back-scatter" is not observed for the unity Prandtl-number case with $Pr = 1$, where q_r^{+C} always evidently remains positive over-compensating the negative Reynolds terms, so that there is not net reduction of the total subgrid-scale flux q_r^+. This aspect will be of importance for the predictions of the scale-similarity based DTM approach discussed below.

MODEL EVALUATION AND DISCUSSION

The four subgrid-scale model concepts discussed above, (i) the constant-coefficient Smagorinsky model (*CSM*), (ii) the dynamic Smagorinsky model (DSM), (iii) the non-linear tensiorial viscosity/diffusivity model (NLM), and (iv) the scale-similarity based dynamic two-parameter model (DTM), were evaluated in *a priori* LES by substituting the grid-filtered DNS-data into the corresponding model formulations. The obtained predictions are always averaged in the homogeneous (azimuthal and axial) directions and compared against the corresponding subgrid-scale contributions as obtained from the grid-filtered non-linear fluxes using the DNS data. For the constant-coefficient Smagorinsky model (*CSM*) a standard parameter setting, $C_S = 0.1$, $A^+ = 26$, and $Pr_T = 0.5$ was used. Figure (5) shows the predicted trace-free axial component of the subgrid-scale stress tensor compared against the filtered DNS-results denoted by the solid line. Since the averages of the normal components of the resolved strain rate tensor are zero in the considered fully developed pipe flow configuration,i.e., $\langle \overline{S}_{rr} \rangle = \langle \overline{S}_{\varphi\varphi} \rangle = \langle \overline{S}_{zz} \rangle = 0$, both the linear eddy-viscosity models, *CSM* and *DSM*, are unable to predict here any normal subgrid-scale stress components like $\tau_{zz}^{+,d}$. The non-linear tensorial-viscosity based extension *NLM* evidently removes this limitation. Due to the scale-similarity contribution in equation (18) the *DTM* describes the normal stress component most accurately, but still with some lack in amplitude around $y^+ = 10$.

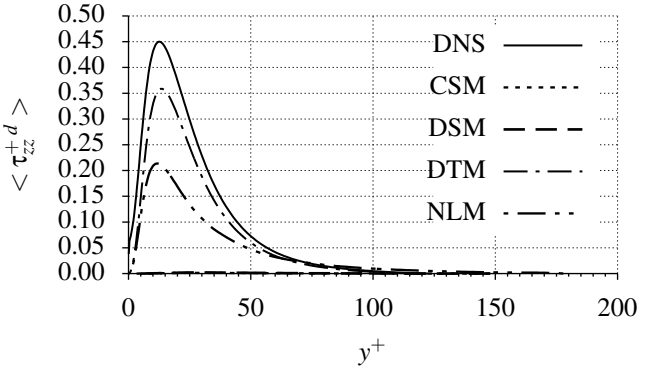

Figure 5. Predicted deviatoric axial subgrid-scale stress $\langle \tau_{zz}^{+,d} \rangle$ compared against filtered DNS results

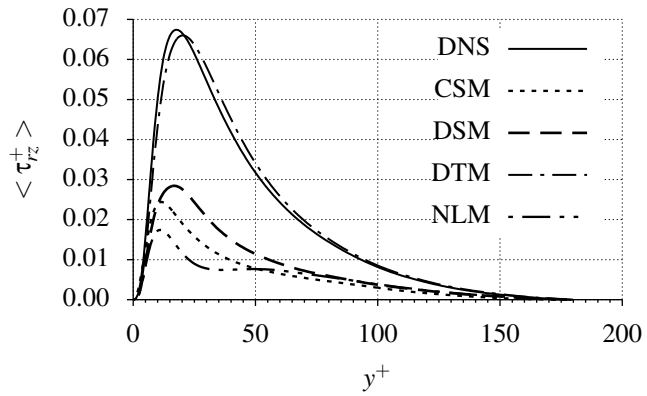

Figure 6. Predicted subgrid-scale shear stress $\langle \tau_{rz}^+ \rangle$ compared against filtered DNS results

Figure (6) shows the predictions for the averaged subgrid-scale shear stress τ_{13}^+. Among the viscosity based model the simplest *CSM* approach is here interestingly the most accurate, while the basically more sophisticated non-linear model (NLM) give the poorest predictions. In contrast, *DTM* approach appears to reproduce the *DNS* results in very close agreement over the whole y^+-range. Figures (7) and (8) show the predicted axial and radial components of the subgrid-scale heat flux, respectively. Analogously to the normal stresses, both linear diffusivity models, *CSM* and *DSM*, are unable to predict any azimuthal and axial heat fluxes, as the averaged resolved gradients into these directions vanish, $\langle \partial \overline{T}/\partial \varphi \rangle = \langle \partial \overline{T}/\partial z \rangle = 0$. Again the *DTM* shows the best agreement with the *DNS* results, although it produces to low maximum values for the axial component q_z^+ near the wall, and this deviation increases with increasing molecular Prandtl number. On the other hand, the near wall maximum of the radial component q_r^+ is predicted very well by the *DTM* approach. With increasing molecular Prandtl number a notable deviation appears in the inner region beyond the near wall maximum. The observed overprediction can be attributed to the fact that the cross flux term is not accounted for using only the scale-similarity based modified Leonard term. The considerable net reduction of the total subgrid-scale heat flux due to the negativity of the cross term as well as the Reynolds term observed for $Pr = 20$ in figure (4) is therefore not reflected by the *DTM* approach. In contrast, the non-linear model (*NLM*) evidently reflects such a back-scattering effect reducing $\langle q_r^+ \rangle$ in this y^+-region, however quantitatively way too strong. The predicted negativity of the total subgrid-scale radial heat flux, $\langle q_r^+ \rangle < 0$, which would imply a net back-scatter of convective heat from the subgrid-scales into the resolved scales, is not supported by the filtered DNS-data. In comparison to the linear diffusivity models the non-linear tensorial extension still enables the (*NLM*) approach to reproduce at least some part of the axial component of the subgrid scale flux fairly well, as seen from figure (7).

Figure (9) shows the variations of the subgrid-scale turbulent Prandtl number as obtained from the dynamic Smagorinky model (*DSM*). It evidently increases towards the wall going farther

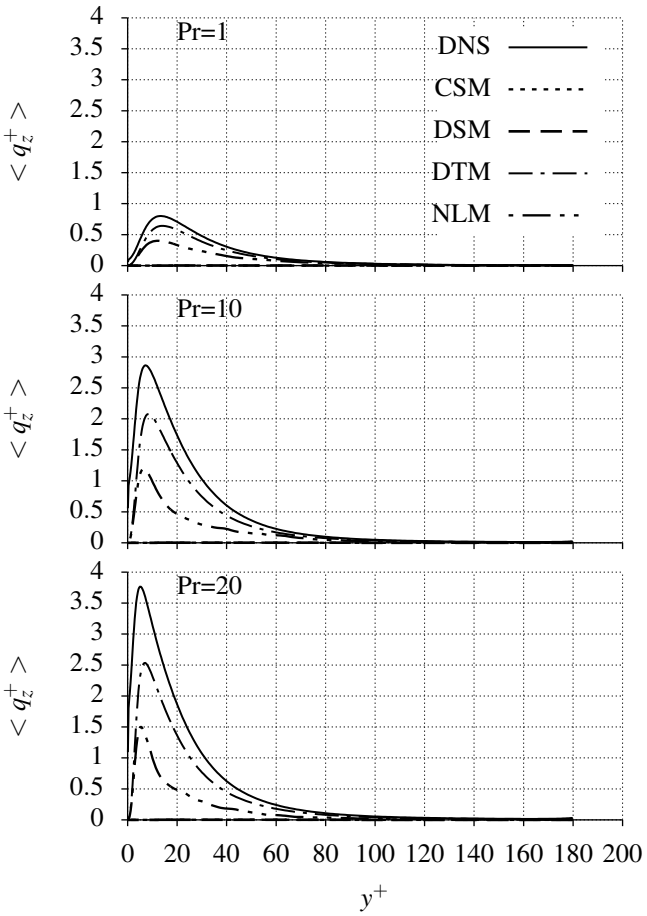

Figure 7. Predicted subgrid-scale axial heat flux $\langle q_z^+ \rangle$ compared against filtered DNS results

beyond unity for increasing molecular Prandtl number. This is basically the same tendency, as observed for the counterpart introduced in the purely statistical RANS-type wall models (see, e.g.,[12]). In the context of RANS the eddy viscosity and eddy diffusivity related by this number represent the complete turbulent motion and not only the unresolved subgrid-scales as in LES. It is further seen that the standard assumption $Pr_T = 0.5$ used by the constant coefficient Smagorinsky model (*CSM*) holds true only for $Pr = 1$ in the core region beyond $y^+ \approx 100$, where the turbulence becomes isotropic. For the higher molecular Prandtl numbers Pr_T evidently requires a higher setting also in the isotropic inner region.

CONCLUSIONS

The present unveils clearly the deficits of the popular constant-coefficient Smagorinsky-type approach mainly due to the observed significant dependence of the subgrid-scale Prandtl number on the molecular Prandtl number. The Germano-type dynamic Smagorinsky model is shown to capture this dependence reasonably well, but it does not substantially improve the predictions of the radial subgid-scale heat flux near the wall as compared to the wall-dampened constant-coefficient version. Unlike the linear Smagorinsky-type models the mathematically elabo-

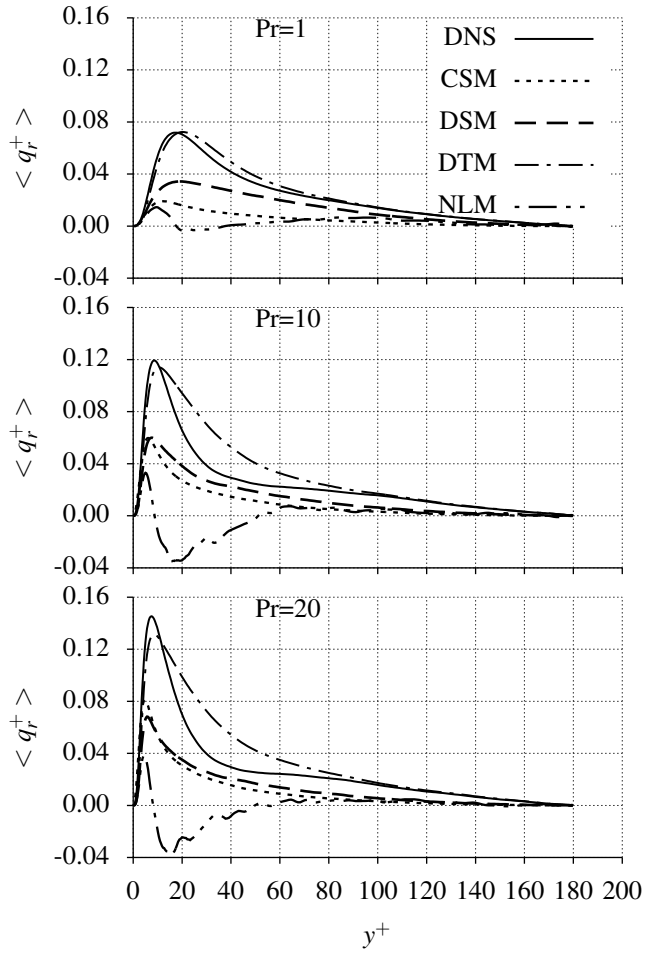

Figure 8. Predicted subgrid-scale radial heat flux $\langle q_r^+ \rangle$ compared against filtered DNS results

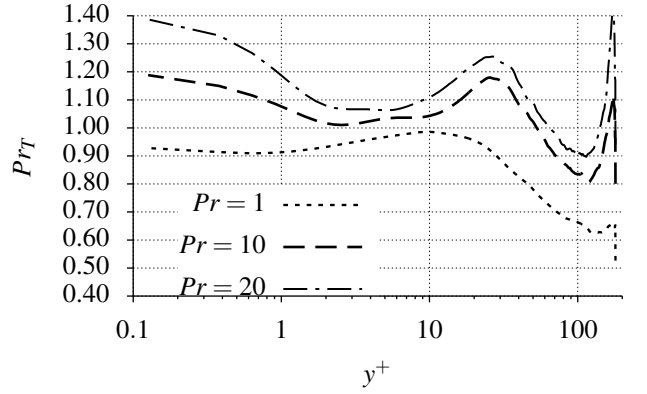

Figure 9. Turbulent subgrid-scale Prandtl number dynamically obtained by the *DSM*

rate non-linear extension proposed by [6] is shown to be able to predict also the axial component, it produces less accurate predictions for the radial component though. In contrast, combining the dynamic Smagorinsky model with the concept of scale-similarity as proposed in the dynamic two parameter model (DTM) by [1] is proven as the most accurate approach. The subgrid-scale contribution of the Leonard term, which is computed from the smallest resolved turbulent fluctuations under the assumption of scale similarity, appears to capture fairly accurate most part of all components of the subgrid-scale stresses and heat fluxes in the core flow region as well as near the wall at all considered molecular Prandtl numbers. Some limitations still appeared with increasing molecular Prandtl number, where the cross term locally drops considerably below zero, effectively reducing the net radial subgrid scale heat flux. Considering presently only the Leonard term the DTM approach should therefore be further developed by including an appropriate submodel for the cross-scale interactions between the resolved and unresolved fluxes to improve its predictive capability for high Prandtl number flow.

ACKNOWLEDGMENTS

The financial support of the Austrian Research Promotion Agency (FFG), the Virtual Vehicle competence center, and AVL List GmbH are gratefully acknowledged.

REFERENCES

[1] Salvetti M.V. and Banerjee S., A priori tests of a new dynamic subgrid-scale model for finite-difference large-eddy simulations. *Physics of Fluids*, 7, 1995, pp. 2831-2847.

[2] Leonard A., Energy cascade in large-eddy simulations of turbulent fluid flows. *Advances in geophysics*, 18, 1975, pp. 237-248.

[3] Smagorinsky J., General circulation experiments with the primitive equations. *Monthly Weather Review*, 91, 1963, pp. 99-164.

[4] van Driest E.R., On Turbulent Flow Near a Wall, *J. Aeronautical Sci.*, Vol. 23, 1956, pp. 1007-1011.

[5] Germano M., Piomelli U., Moin P. and Cabot W.H., A dynamic subgrid-scale eddy viscosity model. *Physics of Fluids A: Fluid Dynamics* (1989-1993), 3, 1991, pp. 1760-1765.

[6] Wang, B.C., Yin J., Yee E. and Bergstrom D.J., A complete and irreducible dynamic SGS heat-flux modelling based on the strain rate tensor for large-eddy simulation of thermal convection. *International Journal of Heat and Fluid Flow*, 28, 2007, pp. 1227-1243.

[7] Bardina J., Ferziger J. H., and Reynolds W.C. Improved turbulence models based on LES of homogeneous incompressible turbulent flow, Department of Mechanical Engineering, *Report No. TF-19*, Stanford, 1984.

[8] Zang Y., Street R.L. and Koseff J.R., A dynamic mixed subgrid-scale model and its application to turbulent recirculating flows. *Physics of Fluids A: Fluid Dynamics*, 5, 1993, pp. 3186-3196.

[9] Nemati H., Patel A., Boersma B.J. and Pecnik R., The effect of thermal boundary conditions on forced convection heat transfer to fluids at supercritical pressure. *Journal of Fluid Mechanics*, 800, 2016, pp. 531-556.

[10] Zonta F., Marchioli C. and Soldati A., Modulation of turbulence in forced convection by temperature-dependent viscosity. *Journal of Fluid Mechanics*, 697, 2012, pp. 150-174.

[11] Lee J., Jung S.Y., Sung H.J. and Zaki T.A., Effect of wall heating on turbulent boundary layers with temperature-dependent viscosity. *Journal of Fluid Mechanics*, 726, 2013, pp. 196-225.

[12] Schwertfirm F. and Manhart M., DNS of passive scalar transport in turbulent channel flow at high Schmidt numbers, *Heat and Fluid Flow 28*, 2007, pp. 1204-1214.